All about FAX: a *F*emale *A*dult vo*X*el phantom for Monte Carlo calculation in radiation protection dosimetry

R Kramer [1], H J Khoury [1], J W Vieira [2,3], E C M Loureiro [3], V J M Lima [4], F R A Lima [5] and G Hoff [6]

[1] Departamento de Energia Nuclear, Universidade Federal de Pernambuco, Av. Prof. Luiz Freire 1000, Cidade Universitária, CEP: 50740-540, Recife, PE, Brazil

[2] Centro Federal de Educação Tecnológica de Pernambuco, Recife, PE, Brazil

[3] Escola Politécnica, UPE, Recife, PE, Brazil

[4] Departamento de Anatomia, Universidade Federal de Pernambuco

[5] Centro Regional de Ciências Nucleares, R. Cônego Barata 999, Recife,PE, Brazil

[6] Faculdade de Física, PUCRS, Porto Alegre, RS, Brazil

E-mail: rkramer@uol.com.br

Statement of provenance:
'This is an author-created, un-copyedited version of an article accepted for publication in Physics in Medicine and Biology. IOP Publishing Ltd is not responsible for any errors or omissions in this version of the manuscript or any version derived from it. The definitive publisher authenticated version is available online at stacks.iop.org/PMB/49/5203 .'

Abstract. The International Commission on Radiological Protection (ICRP) has created a task group on dose calculations, which, among other objectives, should replace the currently used mathematical MIRD phantoms by voxel phantoms. Voxel phantoms are based on digital images recorded from scanning of real persons by computed tomography (CT) or magnetic resonance imaging (MRI). Compared to the mathematical MIRD phantoms, voxel phantoms are true to nature representations of a human body. Connected to a radiation transport code, voxel phantoms serve as virtual humans for which equivalent dose to organs and tissues from exposure to ionizing radiation can be calculated. The principal data base for the construction of the FAX (*F*emale *A*dult vo*X*el) phantom consisted of 151 CT images recorded from scanning of trunk and head of a female patient, whose body weight and height were close to the corresponding data recommended by the ICRP in Publication 89. All 22 organs and tissues at risk, except for the red bone marrow and the osteogenic cells on the endosteal surface of bone ('bone surface'), have been segmented manually with a technique recently developed at the Departamento de Energia Nuclear of the UFPE in Recife, Brazil. After segmentation the volumes of the organs and tissues have been adjusted to reach agreement with the organ and tissue masses recommended by ICRP for the Reference Adult Female in Publication 89. Comparisons have been made with the organ and tissue masses of the mathematical EVA phantom, as well as with corresponding data for other female voxel phantoms. The three-dimensional matrix of the segmented images has eventually been connected to the EGS4 Monte Carlo code. Effective dose conversion coefficients have been calculated for exposures to photons, and compared to data determined for the mathematical MIRD-type phantoms, as well as for other voxel phantoms.

1. Introduction

Phantoms are physical or virtual representations of the human body to be used for the determination of absorbed dose to radiosensitive organs and tissues. In radiation protection a widely used physical model is the ALDERSON-RANDO phantom (Alderson 1962), which consists of a human skeleton embedded in tissue-equivalent material, which has the shape of a human body. Actually the phantom is a pile of 2.5cm thick slices, each of which has a matrix of holes in which small thermoluminescent dosimeters (TLD) can be inserted. Organ and tissue equivalent doses can be determined by averaging over many TLD measurements in a certain volume. However the definition of organ volumes is often difficult because of the irregular shape of organs like the colon, the small intestine, the pancreas, and the stomach, or measurements are simply impossible, like in the case of the red bone marrow. In addition the energy dependence of the TLD response can also complicate the interpretation of measured data, because the energy distribution of the radiation field inside the phantom is usually not known. Finally, using the ALDERSON-RANDO phantom can become a rather troublesome task for the determination of equivalent dose to the 22 radiosensitive organs and tissues which contribute to the effective dose (ICRP 1991).

The development of mathematical heterogeneous human phantoms was essential to overcome these problems. In mathematical human phantoms size and form of the body and its organs are described by mathematical expressions representing combinations and intersections of planes, circular and elliptical cylinders, spheres, cones, tori, etc. By means of radiation transport calculations performed in a mathematical phantom it is possible to register the energy deposited by the radiation in interactions with the atoms of the body tissues. The equivalent dose to a specific organ is determined by dividing the total radiation energy deposited in that organ by its mass, and by multiplying the result by the corresponding radiation weighting factor.

Fisher and Snyder (1967, 1968) introduced this type of phantom for an adult male which also contains ovaries and a uterus. During the compilation of the Report of the Task Group on Reference Man, Publication No.23 (ICRP 1975) the phantom has been further developed by Snyder et al (1974, 1978). Since then it is known as "MIRD-5 phantom" (*M*edical *I*nternal *R*adiation *D*ose Committee (MIRD) Pamphlet No.5).

The MIRD-5 phantom has been the basis for various derivations representing infants and children of various ages (Cristy 1980), gender-specific adult phantoms, called ADAM and EVA (Kramer et al 1982), and a pregnant female adult phantom (Stabin et al 1995). Body height and weight as well as the organ masses of these MIRD-type phantoms are in accordance with the Reference Man data from 1975 (ICRP 1975).

Although facilitating significantly the task of equivalent dose determination, the mathematical MIRD5-type phantoms are still rather stylized models of the human body and its organs. This problem has been resolved by the development of tomographic or voxel(-based) phantoms. Voxel phantoms are based on digital images recorded from scanning of real persons by computed tomography (CT) or magnetic resonance imaging (MRI). Each image consists of a matrix of pixels (picture elements), whose number depends on the resolution chosen during scanning. A consecutive set of such images can be considered as a three-dimensional matrix made of voxels (volume pixels), where each voxel belongs to a specific organ or tissue. Compared to the mathematical phantoms, voxel phantoms are true to nature representations of human bodies.

Tomographic or voxel phantoms have been introduced by Gibbs et al (1984) and independently also by Williams et al (1986), who extended this effort to construct infant and children voxel phantoms (Veit et al 1989) as well as a "voxelized" version of the Alderson-Rando phantom

(Veit et al 1992). Meanwhile these activities have produced a whole family of voxel phantoms (Petoussi-Henss et al 2002, Fill et al 2004).

Zubal et al (1994a, 1994b, 1995) segmented CT and MRI data of a patient who was scanned from head to mid-thigh. Dimbylow (1995) introduced the voxel phantom NORMAN based on MRI data of a healthy volunteer. The voxel dimensions of NORMAN have been scaled to match body height and weight of the first Male Reference Adult (ICRP 1975), that is a body weight of 70kg and a body height of 170cm.

Caon et al (1997, 1999) developed a voxel phantom of a 14 year old girl, Saito et al (2001) segmented whole-body CT data of a patient whose external dimensions were in good agreement with the Japanese Reference Man (Tanaka 1989), and Xu et al (2000) segmented color photographs of the Visible Human Male (Spitzer and Whitlock 1998) for the construction of the VIPMAN voxel phantom. Comprehensive reviews on the development of voxel-based anthropomorphic phantoms can be found in articles published by Lemosquet et al (2003) and Coan (2004).

Based on data published by Zubal (2001) on a website of the YALE University, Kramer et al (2003) developed the MAX (*M*ale *A*dult vo*X*el) phantom which corresponds anatomically to the specifications of the revised Male Reference Adult, published by the ICRP in Report No.89 (ICRP 2003).

This paper presents the development of the FAX (*F*emale *A*dult vo*X*el) phantom based on CT images of female patients. Similar to the development of the MAX phantom, the organ and tissue masses of the FAX phantom have been adjusted in order to correspond to the anatomical specifications defined by the ICRP for the Female Reference Adult (ICRP 2003). The article presented here represents the revised and extended version of a preliminary publication about the FAXht (head+trunk) phantom (Loureiro et al 2004).

2. Materials and methods

2.1 Data base

The main set of data used for the construction of the FAX phantom consisted of 151 consecutive CT images of a 37 year old female patient. The patient's height was 165cm, and her weight was 63.4kg. The images covered the trunk, the neck and the lower part of the head including the mandible with the lower teeth. The pixel size was 0.073cm x 0.073cm, and the distance between two consecutive images was 0.5cm. The images had been provided by CT Screening International, Irvine, CA92612, USA in October 2002.
A second set of data consisted of 206 consecutive CT images of the legs and feet of a 62 year old woman. The pixel size was 0.07cm x 0.07cm, and the distance between two consecutive images was 0.25cm. The images had been provided by the university hospital of the city of Porto Alegre, Brazil in September of 2003.

2.2 Segmentation

The CT images of the patients have been obtained in the format DICOM (Digital Imaging and Communications in Medicine), and have been visualized by means of the software OSIRIS (Ligier et al 1994), which is available on the internet. OSIRIS has several types of filters which allow improving the visualization of boundaries between organs. After editing the images have

been saved as BitMap files with the software PAINT, which is included in the Microsoft WINDOWS accessories.

Segmentation was done in each of the 357 images with PAINT by manually painting every organ and tissue of interest with a different color (Loureiro 2002). Thereby the grey values of the pixels which belong to a specific organ were replaced by a specific color, which corresponds to a specific number. At the end of the procedure the pile of images represented a three-dimensional voxel matrix, in which all voxels of a specific organ or tissue have the same identification number. According to the definition of the effective dose (ICRP 1991) the following organs and tissues have been segmented: Adrenals, bladder wall, skeleton, brain, breasts, colon, kidneys, liver, lungs, muscle, oesophagus, ovaries, pancreas, small intestine, skin, spleen, stomach, thymus, thyroid, trachea, and uterus. Although not included in the effective dose, the heart and adipose tissue have also been segmented. A description of the representation of the red bone marrow is given in section 2.7.

2.3 Addition of head and arms

In the preliminary version of the FAXht phantom (Loureiro 2004) the upper part of the head was supplemented with images taken from the VOXELMAN phantom (Zubal 2001). However it was found that only a complete set of images from one and the same head would give a anatomically satisfying representation. Therefore, and for practical reasons the head of the MAX phantom was attached to the neck of the FAX phantom, after scaling down the MAX phantom's head according to the anatomical differences between the Male and the Female Reference Adult as defined by ICRP89 (ICRP 2003). The same procedure was applied to the addition of the arms, which also have been taken from the MAX phantom.

2.4 Anatomical corrections

During screening the patient was asked to raise the arms behind her head. Therefore the shoulders and the upper part of the arms have been re-designed according to data from anatomical text books. The images of the trunk, the head, the arms and the legs originated from three different patients. Therefore, with respect to the representation of the skeleton some adjustments had to be made again based on anatomical textbooks, but at the same time also taking into account as much as possible the reference distribution of bone mass fractions given by ICRP89 (ICRP 2003). The form of the breasts has also been modified in order to represent an upright standing adult female. Finally all segmented images have been resampled to achieve the same voxel size of 0.36cm x 0.36cm x 0.36cm = 0.046656cm^3 as in the case of the MAX phantom, and the total number of slices has been adjusted to 453, which corresponds to a body height of 163cm.

2.5 Adjustment of organ and tissue masses

The organ and tissue masses of the Female Reference Adult are defined by ICRP89 (ICRP 2003). Applying the ICRU44 tissue densities (ICRU 1989) shown in Table 1, the corresponding organ volumes have been determined. The composition and density of soft tissue has been averaged from the data for brain, breasts, colon, heart, kidneys, liver, pancreas, spleen, ovaries and thyroid. Division of these volumes by 0.046656 cm^3 yields the number of voxels contained in each organ and tissue. Accordingly the actual voxel numbers of the organs have been increased or decreased until the desired voxel number was realized. As practically all organs are surrounded by adipose and/or muscle tissue, the procedure of adjustment actually consisted of

exchanging ID numbers between voxels of a specific organ with those of surrounding adipose or muscle tissue.

Table 1. Tissue compositions and densities based on ICRU44

Atomic No.	1	6	7	8	11	12	15	16	17	19	20	26	53	Density
Symbol	H	C	N	O	Na	Mg	P	S	Cl	K	Ca	Fe	I	
	[%]	[%]	[%]	[%]	[%]	[%]	[%]	[%]	[%]	[%]	[%]	[%]	[%]	[g/cm^3]
SOFT TISS	10,5	12,5	2,6	73,5	0,2		0,2	0,18	0,22	0,21	0,01	0,01	0,01	1,05
ADIPOSE	11,4	59,8	0,7	27,8	0,1			0,1	0,1					0,95
LUNG	10,3	10,5	3,1	74,9	0,2		0,2	0,3	0,3	0,2				0,26
MUSCLE	10,2	14,3	3,4	71	0,1		0,2	0,3	0,1	0,4				1,05
SKIN	10	20,4	4,2	64,5	0,2		0,1	0,2	0,3	0,1				1,09
CARTILAGE	9,6	9,9	2,2	74,4	0,5		2,2	0,9	0,3					1,1
BONE	3,4	15,5	4,2	43,5	0,1	0,2	10,3	0,3			22,5			1,92
RED BM	10,5	41,4	3,4	43,9			0,1	0,2	0,2	0,2		0,1		1,03
YELL BM	11,5	64,4	0,7	23,1	0,1			0,1	0,1					0,98

BM = bone marrow

2.6 Dosimetry for the skin

Based on data given by ICRP89 (ICRP 2003) an average thickness of 1.2mm for the female skin was calculated. Similar to the procedure applied to the MAX phantom (Kramer et al 2003), instead of sub-segmenting the 3.6mm surface voxel layer, equivalent dose to the first 1.2mm skin depth will be calculated by 'dosimetric separation' within the 3.6mm voxel thickness. Depending on the location of the radiation interaction in the first voxel layer, the energy lost by the particle will be deposited either within the 1.2mm superficial skin layer, or within the underlying 2.4mm of adipose tissue.

2.7 Skeletal tissue distribution

Segmentation of the red bone marrow (RBM) within trabecular bone requires CT images with pixel sizes in the micrometer range. For selected bone samples progress has been made in the area of RBM segmentation (Bolch et al 2002), but for the time being such pixel resolutions for a complete human skeleton are still not available. Therefore whole-body RBM dosimetry still has to be based on the calculation of the radiation energy deposited in a homogeneous mixture of bone, marrow and cartilage to which then certain correction factors are applied.
While in the mathematical phantoms (Kramer et al 1982) only one specific homogeneous skeletal mixture was used for the whole skeleton, in voxel phantoms it is possible to create a heterogeneous skeletal tissue distribution throughout the bones by assigning specific mixtures to each skeletal voxel. This is done with the CT number method (Zankl and Wittman 2001) as adopted by Kramer et al (2003), which uses the grey values of bone pixels in the original CT images of the scanned patient to establish voxel-specific tissue distributions of bone, marrow and cartilage. An extensive description of RBM dosimetry based on the CT number method has been given in the publication of the MAX phantom (Kramer et al 2003). Therefore this chapter will present mainly those data which are specific for the FAX phantom.

Table 2. Female skeletal tissue distribution based on ICRP89

TISSUE	MASS	DENSITY	VOLUME	VOLUME
	g	g/cm^3	cm^3	FRACTION
BONE	4000	1.92	2083.3	0.361
RED BM	900	1.03	873.8	0.151
YELL BM	1800	0.98	1836.7	0.318
CARTILAGE	900	1.10	818.2	0.142
MISC.	200	1.20	166.7	0.029
TOTAL	7800		5778.7	1.000

BM = bone marrow, MISC. = teeth, periosteum, and blood vessels

Column 2 of table 2 shows the ICRP89 reference masses (ICRP 2003) for bone, RBM, yellow bone marrow, cartilage and miscellaneous tissues. With the densities from table 1 it is possible to calculate the corresponding volumes to be seen in column 4, and finally to determine the volume fractions for each skeletal tissue shown in the last column. The density for the miscellaneous tissues has been assessed based on data given by ICRP70 (ICRP 1995).

The volume of a skeleton with a tissue distribution based on ICRP89 contains ca. 17% of cartilage plus miscellaneous tissues. During the segmentation of CT images cartilage is usually segmented sometimes as part of bone and sometimes as part of skeletal muscle in order to achieve smooth surfaces between the skeleton and the surrounding muscle tissue. This also happens with the periosteum and the connected blood vessels, which are mostly located on the surface of bone. It was therefore decided to include only half of that volume, or 8.5%, in the skeletal tissue distribution of the FAX skeleton. The teeth, representing only 0.3% of the total skeletal volume, are already part of the segmented bone volume, and have therefore been neglected for further explicit considerations.

After segmentation and adjustment of the bone masses, the skeleton of the FAX phantom turned out to consist of 119938 voxels, which correspond to a volume of 119938 x $0.04666cm^3$ = 5596 cm^3. The mass of the RBM becomes therefore $5596cm^3$ x 0.151 x $1.03gcm^{-3}$ = 870g, where 0.151 represents the volume fraction shown in table 2. This mass has to be distributed among the various bones of the skeleton. However, this distribution has to take into account additional information provided by ICRP70. Table 3 shows the cellularity factors, which indicate the percentage of bone marrow volume occupied by the haematopoietic cells of the RBM, and the mass of RBM in a specific bone (group) as a percentage of the total RBM mass.

Table 3. Cellularity factors and percentage mass fraction of RBM from ICRP70

Specific Bone	Cellularity Factor	RBM mass [%]
Lower Arms	0	0
Upper Arms	0.25	2.3
Ribcage*	0.60	22.8
Spine/Sacr.	0.70	42.2
Skull/Mand.	0.38	8.4
Pelvis	0.48	17.5
Upper Legs	0.25	6.7
Lower Legs	0	0

* Ribs, sternum, clavicles, scapulae

Following the CT number method, grey values in the range between 0 and 255 contained in the bone pixels of the original CT images have been used to establish a heterogeneous tissue distribution throughout the skeleton consisting of marrow, marrow-bone-cartilage, and bone-cartilage voxels. The amount of RBM in the marrow-containing voxels was determined by use of the cellullarity factors. The CT number ranges for the three types of skeletal voxels have been chosen in such a way that the resulting RBM mass fractions match the corresponding ICRP data from table 3 as closely as possible, and that at the same time a total RBM mass of 870g was achieved.

3. Results

3.1 Organ and tissue masses

Table 4 summarizes the 22 radiosensitive female organs and tissues which are included in the definition of the effective dose plus adipose for the Female Reference Adult (ICRP 2003), for the GSF mathematical EVA phantom (Kramer et al 1982), for the adult female GSF voxel phantoms DONNA, HELGA, IRENE (Zankl et al 2002a), and for the FAX phantom. The last column shows the percentage difference between the masses for the FAX phantom and the Female Reference Adult.

Table 4. Organ and tissue masses for the Female Reference Adult and various phantoms

		Math. Phant.	Female Adult Voxel Phantoms				
	ICRP89	GSF	GSF	GSF	GSF	UFPE	Perc. Diff.
ORGAN/TISSUE	Female Ref.	EVA	DONNA	HELGA	IRENE	FAX	FAX/Fem.Ref.
	[g]	[g]	[g]	[g]	[g]	[g]	[%]
Adipose (Fat)	18000		34820	39800	11630	18175	+1.0
Adrenals	13	12.9	21.7	6.6	12.4	13	0
Bladder wall	40	45	61	60.8	39	40	0
Skeleton	7800	8360	7484	6503	8201	8084	+3.6
Brain	1300	1120	1208	1279	1255	1300	0
Breasts	500	532	43.9*	134*	57*	500	0
Colon	680	600	322	426	271	680	0
Kidneys	275	236	281	390	212	275	0
Liver	1400	1471	1585	1757	1225	1400	0
Lung	950	830	631	463	685	950	0
Muscle,skeletal	17500		25420	21340	21100	17500	0
Oesophagus	35	39.7	27.7	28	24.3	35	0
Ovaries	11	10.9	12.1	11.9	11.9	11	0
Pancreas	120	79.6	41.2	43.3	61.9	120	0
Red BM	900	1246	1012	1043	916	870	-3.3
Small Intestine	880	894	435	443	396	880	0
Skin	2300	2803	4351	1653	3620	2302	+0.1
Spleen	130	144	306	298	203	130	0
Stomach	370	125.3	500	73.1	368	370	0
Thymus	20	20	19	7.7	25.3	20	0
Thyroid	17	16.4	18.7	31.5	20	17	0
Trachea	8					8	0
Uterus	80	80	71.7	79.8	25	80	0
Total Body	60000	59193	79000	81000	51000	59762	-0.4
Height	163 cm	160cm	176cm	170cm	163cm	163cm	0

Colon, Small Intestine and Stomach include contents, * = only glandular tissue; GSF = Research Center for Environment and Health, Munich, Germany; UFPE = Universidade Federal de Pernambuco, Recife, Brazil.

Most organ and tissue masses of the FAX phantom have values recommended by ICRP89. However, the RBM mass is 3.3% smaller than the reference mass, because with 5596cm^3 the volume of the FAX skeleton is ca. 3.3% smaller than the reference volume shown in table 3. Nevertheless the mass of the FAX skeleton is by about the same margin greater than the reference mass, which is due to the average density of 1.445gcm^{-3} of the FAX skeleton calculated by the CT number method, while on the other hand table 3 would suggest an average skeletal density of only 7800g / 5778.7cm^3 = 1.35gcm^{-3}. As already pointed out elsewhere (Kramer et al 2003) average skeletal densities published by the ICRP (ICRP 1975, 1995, 2003) vary between 1.3 – 1.4g cm^{-3}, while for voxel phantoms the reported values are usually greater than 1.4gcm^{-3} (Chao et al 2001, Zankl 2002b, Kramer et al 2003).

Comparisons of organ and tissue masses between FAX and the other female voxel phantoms do not make a lot of sense, because the masses for DONNA, HELGA, and IRENE have not been changed to match the reference values. Indeed with regard to dosimetry it is more interesting to compare equivalent doses to organs and tissues for different phantoms, but in this case not only different masses but also different tissue compositions, organ locations and positions would influence the equivalent doses (Kramer et al 2004).

3.2 Bone mass adjustment and RBM distribution

Table 5 shows the mass fractions of bone for the Female Reference Adult and for the FAX phantom. The average deviation from the reference values is less than 6%.

Table 5. Fractions of total fresh skeletal mass contributed by various bones, including bone marrow for the Female Reference Adult (ICRP 2003) and the FAX phantom

Specific Bone	ICRP89 mass fract.	FAX mass fract.
Lower Arms	0.056	0.056
Upper Arms	0.047	0.054
Ribcage*	0.104	0.106
Spine/Sacr.	0.204	0.197
Skull/Mand.	0.131	0.147
Pelvis	0.106	0.109
Upper Legs	0.159	0.148
Lower Legs	0.193	0.183

* Ribs, sternum, clavicles, scapulae

Column 3 of table 6 shows the percentage mass fractions of RBM achieved for the FAX phantom after distributing 870 g of RBM throughout the skeleton by the CT number method, after taking into account the cellularity factors of table 4, and after "tuning" the skeletal tissue distribution to approximate the ICRP RBM mass fraction shown in tables 3 and 6. Like for the MAX phantom (Kramer et al 2003) the average deviation from the reference data is ca. 1%. The last column of table 6 presents for comparison the RBM mass fractions of the mathematical ADAM and EVA phantom (Kramer et al 1982), which are based on the data from the first Reference Man Report published in ICRP 23 (ICRP 1975).

Table 6. Percentage mass fractions of RBM for the Female Reference Adult and various phantoms

	ICRP70	FAX	MAX	ADAM/EVA
Bone	[%]	[%]	[%]	[%]
Lower Arms	0	0	0	0
Upper Arms	2.3	3.0	3.6	1.9
Ribcage*	22.8	21.7	23.0	16.6
Spine/Sacr.	42.2	43.6	42.7	28.4
Skull/Mand.	8.4	8.4	7.7	13.1
Pelvis	17.5	16.6	16.3	36.2
Upper Legs	6.7	6.7	6.7	3.8
Lower Legs	0	0	0	0
Total	99.9	100.0	100.0	100.0

* Ribs, sternum, clavicles, scapulae

3.3 Images of the FAX phantom

Figure 1 shows a frontal and a lateral view of the FAX phantom. Apart from the skeleton, most of the segmented organs can be seen. 3D views of the FAX phanotm's surface are shown in Figure 2.

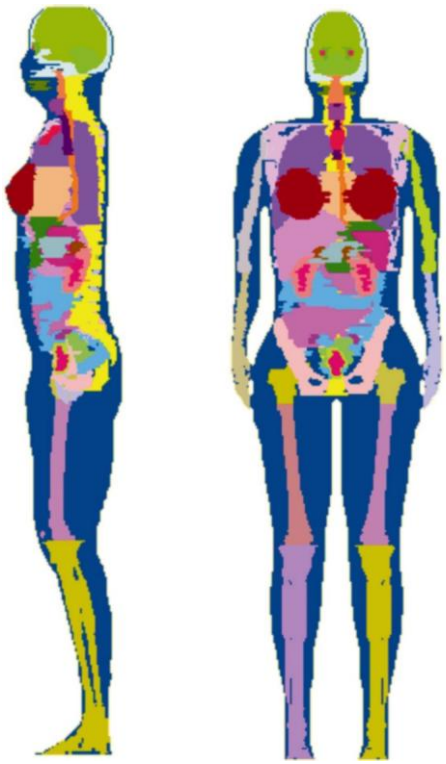

Figure 1. The FAX phantom: Frontal and lateral view with skeleton and internal organs

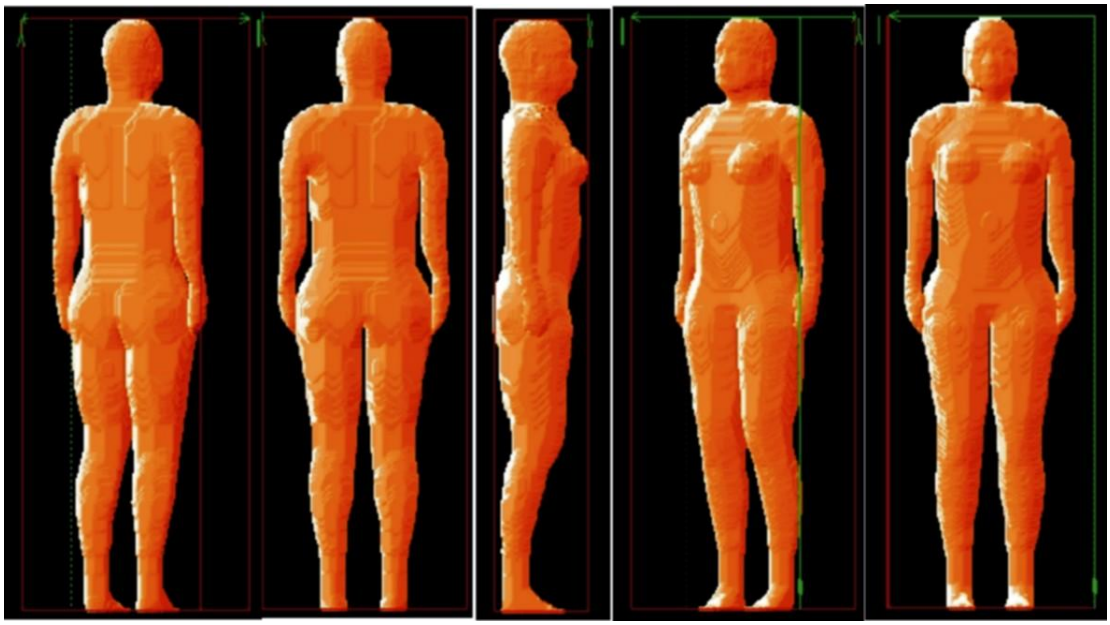

Figure 2. The FAX phantom: 3D views for different projections

3.4 Effective dose

Although mainly concerned with the development of the FAX phantom, this paper will give a preview on dosimetric data currently being calculated for a comprehensive publication of effective dose conversion coefficients.

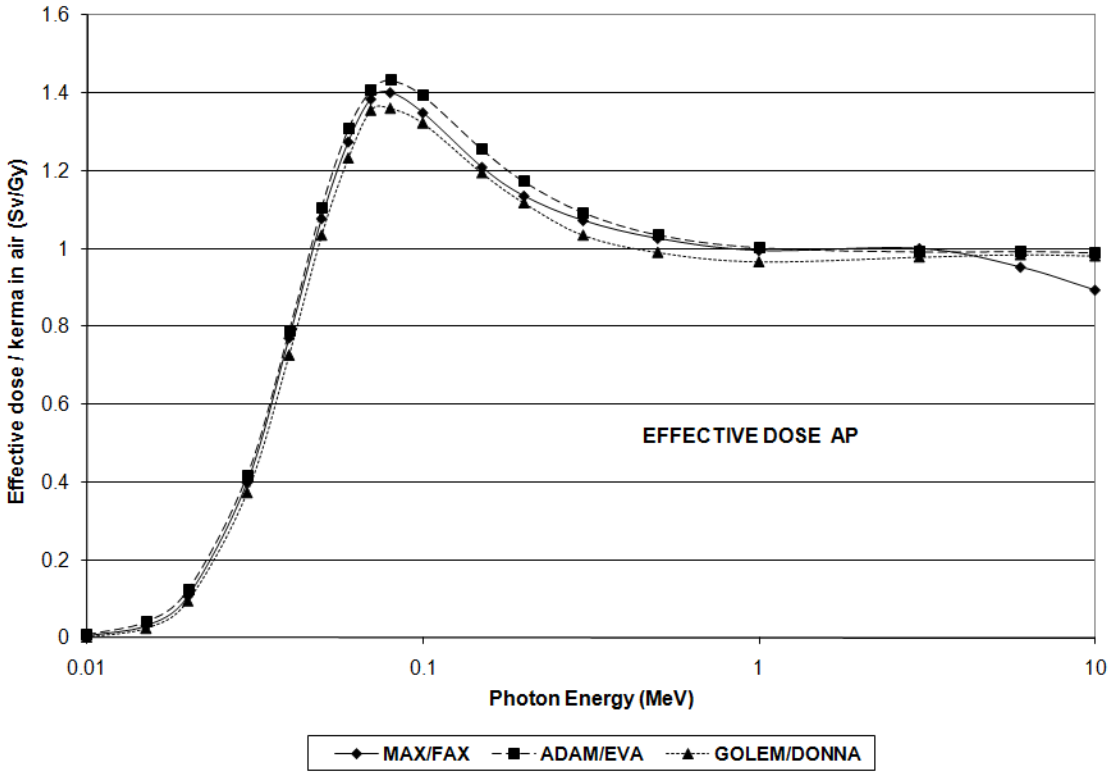

Figure 3. Conversion coefficients between effective dose and air kerma free-in-air for external exposure to photons as a function of incident energy for the MAX/FAX, the ADAM/EVA, and the GOLEM/DONNA phantoms: AP incidence

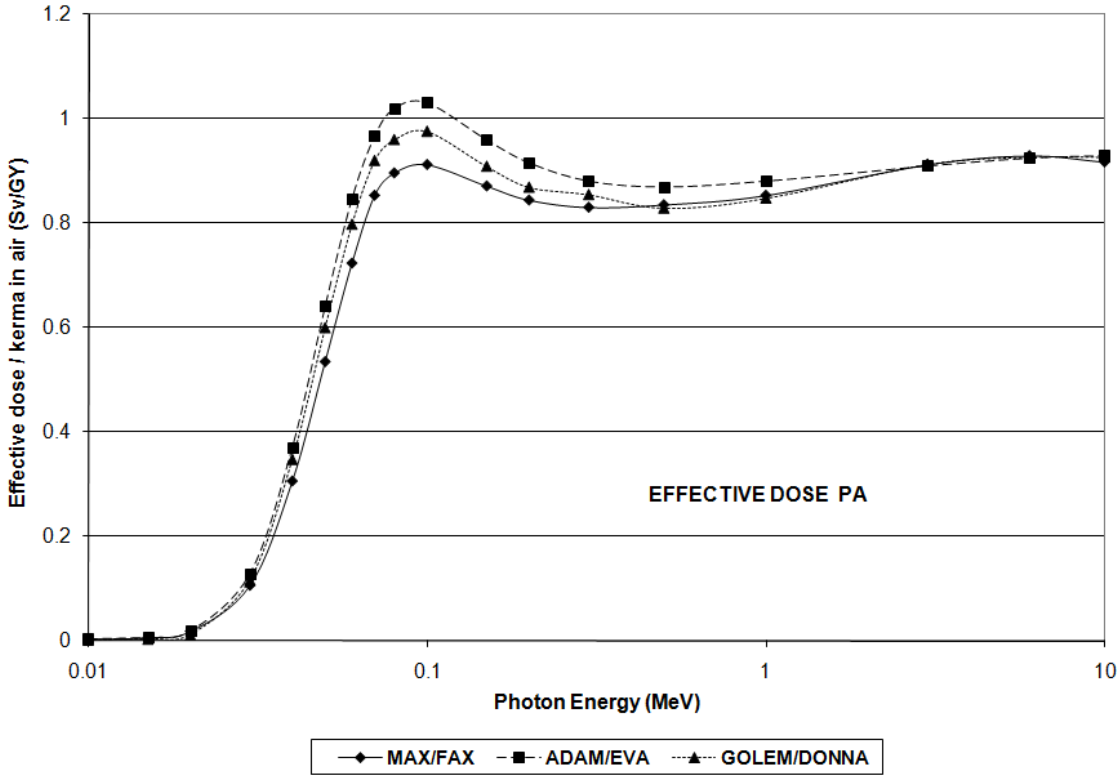

Figure 4. Conversion coefficients between effective dose and air kerma free-in-air for external exposure to photons as a function of incident energy for the MAX/FAX, the ADAM/EVA, and the GOLEM/DONNA phantoms: PA incidence

The MAX and the FAX phantoms, the first pair of ICRP89-based adult human models, have been exposed to a parallel beam of monoenergetic photons which covered the whole body for energies between 10 keV and 10 MeV. For frontal exposure (AP) figure 3 shows the effective dose normalized to air kerma free-in-air as a function of the incident photon energy, while figure 4 presents the same conversion coefficient for exposure from the back (PA).

Effective doses for the mathematical ADAM and EVA phantoms (Zankl et al 1997), as well as for the GOLEM and DONNA voxel phantoms (Zankl et al 2002c) are also shown for comparison.
Compared to the mathematical ADAM and EVA phantoms the effective dose for the MAX and FAX voxel phantoms is always smaller over the whole range of energies, and for both directions of incidence. The main reasons for the decrease of the "voxel effective dose" compared to the "MIRD effective dose" for external whole body photon irradiation are

a) that in real human bodies most of the radiosensitive organs experience more shielding by the skeleton and/or by muscle tissue than in the bodies of the mathematical phantoms (Kramer et al 2004), and
b) that especially for the MAX and FAX voxel phantoms the equivalent dose to the RBM is significantly smaller, because of the revised RBM mass fractions (ICRP 2003), the updated photo-electron correction factors (King and Spiers 1985), and the calculation of the energy deposited per interaction in voxel-specific skeletal tissue distributions based on CT numbers from the original images of the scanned patient (Kramer et al 2003).

These findings are also supported by the effective dose conversion coefficients for the GOLEM and the DONNA voxel phantoms, which are also always smaller than the corresponding data for the mathematical phantoms ADAM and EVA.
Analysis of equivalent doses for the MAX, FAX, GOLEM, and DONNA voxel phantoms for the organs and tissues with the greatest weighting factors reveal that the data show similar values for the colon, the lungs, and the stomach, but not for the ovaries, the testes, and the RBM. For AP incidence the ovaries equivalent dose is greater for the FAX than for the DONNA phantom because of different positions and different body thicknesses, and the testes equivalent dose is greater for the MAX than for the GOLEM phantom because the closed thighs of the MAX phantom produce backscatter radiation, while the open thighs of the GOLEM phantom do not. The RBM equivalent dose is moderately greater for the GOLEM and the DONNA phantoms than for the MAX and the FAX phantoms because different calculational methods are applied (Kramer et al 2003), but finally the effective dose for MAX and FAX is greater than for GOLEM and DONNA.
Due to the anatomical differences with respect to the thighs, for PA incidence the testes equivalent dose is now greater for the GOLEM phantom than for the MAX phantom. For PA incidence the ovaries equivalent dose is now significantly greater for the DONNA phantom than for the FAX phantom for the reasons already mentioned. The RBM equivalent dose is again greater for the GOLEM and DONNA phantoms. Therefore for PA incidence the effective dose is greater for the GOLEM and DONNA phantom than for the MAX and FAX phantoms.

4. Conclusion

CT images from female patients have been segmented with respect to the organs and tissues of the human body considered relevant by ICRP for the calculation of the effective dose. The segmented images have been assembled to form a three-dimensional voxel matrix, called FAX phantom.
The masses of all relevant organs and tissues have been adjusted to match the reference values given by ICRP89 for the Female Reference Adult. Using skeletal tissue data from ICRP70 and ICRP89 it was possible to determine the RBM mass which corresponds to the segmented volume of the FAX skeleton. Application of the CT number method and consideration of the cellularity factors made it possible to realize a RBM distribution in a heterogeneous skeleton close to the RBM mass fractions given by ICRP70.

Together with the earlier developed MAX phantom it is now possible to calculate the effective dose for a pair of a female and a male voxel phantom, which correspond in their anatomical specifications to the reference data given by ICRP89.
Information about the use of the voxel phantoms MAX and FAX by members of the scientific community can be obtained from the email address mentioned above.

5. Acknowledgement

The authors would like to thank CNPq and FACEPE for the financial support, and especially Dr.med. A.Kramer for critically reviewing the overall body design of the FAX phantom.

6. References

Alderson S W, Lanzl L H, Rollins M and Spira J (1962) An instrumented phantom system for analog computation of treatment plans. Am. J. Roentg. 87, 185

Bolch W E, Patton P W, Rajon D A, Shah A P, Jokisch D W, Inglis B A (2002), Consideration Of Marrow Cellularity in 3-Dimensional Dosimetric Models of the Trabecular Skeleton, J Nucl Med, 43:97-108

Caon M, Bibbo G and Pattison J (1997) A comparison of radiation dose measured in CT dosimetry phantoms with calculations using EGS4 and voxel-based computational models. Phys. Med. Biol. **42**:219-229

Caon M, Bibbo G and Pattison, J. (1999) An EGS4-ready tomographic computational model of a fourteen-year-old female torso for calculating organ doses from CT examinations. Phys. Med. Biol. **44**:2213-2225

Caon M (2004) Voxel-based computational models of real human anatomy: a review. Radiat. Environ. Biophys. **42**:229-235

Chao T C, Bozkurt A, Xu X G (2001a), Conversion Coefficients Based on the VIP-Man Anatomical Model and EGS4-VLSI Code for External Monoenergetic Photons from 10 keV to 10 MeV, Health Physics 81(2):163-183

Cristy M (1980) Mathematical phantoms representing children at various ages for use in estimates of internal dose. Report ORNL/NUREG/TM-367, Oak Ridge National Laboratory, Oak Ridge, Tenn., USA

Dimbylow P J (1995) The development of realistic voxel phantoms for electromagnetic field dosimetry. In: Proceedings of an International Workshop on Voxel Phantom Development held at the National Radiological Protection Board, Chilton, UK, 6-7 July

Fill U A, Zankl M, Petoussi-Henss N, Siebert M and Regulla D (2004) Adult Female Voxel Models of Different Stature and Photon Conversion Coefficients for Radiation Protection. Health Phys. **86**(3): 253-272

Fisher H L and Snyder W S (1967) Distribution of dose in the body from a source of gamma rays distributed uniformly in an organ. Report No. ORNL-4168, Oak Ridge National Laboratory, Oak Ridge, Tenn., USA

Fisher H L and Snyder W S (1968) Distribution of dose in the body from a source of gamma rays distributed uniformly in an organ. In: Proceedings of the First International Congress on Radiation Protection, Pergamon Press, Oxford, pp 1473-1486

Gibbs S J, Pujol A, Chen T S, Malcolm A W and James A E (1984) Patient risk from interproximal radiography. Oral Surg. Oral Med. Oral Pathol., **58**:347-354

ICRP (1975) Report of the Task Group on Reference Man. ICRP Publication 23, International Commission on Radiological Protection, Pergamon Press, Oxford

ICRP (1991) 1990 Recommendations of the International Commission on Radiological Protection. ICRP Publication 60. International Commission on Radiological Protection, Pergamon Press, Oxford

ICRP (1995), Basic Anatomical and Physiological Data for use in Radiological Protection: The Skeleton. ICRP Publication 70.International Commission on Radiological Protection, Pergamon Press, Oxford

ICRP (2003) Basic Anatomical and Physiological Data for Use in Radiological Protection: Reference Values. ICRP Publication 89, International Commission on Radiological Protection, Pergamon Press, Oxford

ICRU (1989), Tissue substitutes in radiation dosimetry and measurement. ICRU Report 44. International Commission on Radiation Units and Measurements, Bethesda, MD

King S D, Spiers F W (1985), Photoelectron enhancement of the absorbed dose from X rays to human bone marrow: experimental and theoretical studies, Br. J. of Radiol. **58**, 345-356

Kramer R, Zankl M, Williams G and Drexler G (1982) The Calculation of Dose from External Photon Exposures Using Reference Human Phantoms and Monte Carlo Methods. Part I: The Male (ADAM) and Female (EVA) Adult Mathematical Phantoms. GSF-Report S-

885.Reprint July 1999.Institut fuer Strahlenschutz, GSF-Forschungszentrum fuer Umwelt und Gesundheit, Neuherberg-Muenchen

Kramer R, Vieira J W, Khoury H J, Lima F R A and Fuelle D (2003) All About MAX: A *M*ale *A*dult Vo*X*el Phantom for Monte Carlo Calculations in Radiation Protection Dosimetry, Phys. Med. Biol., **48**, No.10, 1239-1262

Kramer R, Vieira J W, Khoury H J, and Lima F R A (2004) MAX meets ADAM: A dosimetric comparison between a voxel-based and a mathematical model for external exposure to photons. Phys.Med.Biol. **49,** 887-910

Lemosquet A, de Carlan L and Clairand I (2003) Voxel anthropomorphic phantoms: review of models used for ionising radiation dosimetry. Radioprotection **38**(4): 509-528

Ligier Y, Ratib O, Logean M and Girard C (1994) Osiris: a medical image manipulation system. M. D. Comput. J., **11**(4): 212-218

Loureiro E C M, Lima F R A and Stabin M (2002) A voxel-based head-and-neck phantom built from tomographic colored images. Cell Mol Biol **48**(5):46104-464

Loureiro E C M, Kramer R, Vieira J W, Khoury H, Lima F R A and Hoff G (2004) Construction of the FAXht (Female Adult voXel) head+trunk phantom from CT images of patients for applications in radiation protection. Paper presented at the 11th International Congress of the International Radiation Protection Association, 23.-28.5.2004, Madrid, Spain

Petoussi-Henss, N, Zankl M, Fill U and Regulla D (2002) The GSF family of voxel phantoms. Phys. Med. Biol**. 47**:89-106

Saito K, Wittmann A, Koga S, Ida Y, Kamei T, Funabiki J and Zankl M (2001) Construction of a computed tomographic phantom for a Japanese male adult and dose calculation system. Radiat Environ Biophys **40**: 69-76

Snyder W S, Ford M R, Warner G G and Watson G G (1974) Revision of MIRD Pamphlet No. 5 Entitled "Estimates of absorbed fractions for monoenergetic photon sources uniformly distributed in various organs of a heterogeneous phantom". ORNL-4979, Oak Ridge National Laboratory, Oak Ridge, Tenn.

Snyder W S, Ford M R and Warner G G (1978) Estimates of absorbed fractions for monoenergetic photon sources uniformly distributed in various organs of a heterogeneous phantom. MIRD Pamphlet No.5, revised, Society of Nuclear Medicine, New York N. Y.

Spitzer V M and Whitlock D G (1998) Atlas of the visible human male. Jones and Bartlett, Boston, Mass., USA

Stabin M, Watson E, Cristy M, Ryman J, Eckerman K, Davis J, Marshall D and Gehlen K (1995) Mathematical models and specific absorbed fractions of photon energy in the nonpregnant adult female and at the end of each trimester of pregnancy. Report No. ORNL/TM-12907, Oak Ridge National Laboratory, Oak Ridge, Tenn., USA

Tanaka G, Nakahara Y and Nakajima Y (1989) Japanese Reference Man 1988-IV: studies on the weight and size of internal organs of normal Japanese. Nippon Igaku Hoshasen Gakkai Zasshi **49**:344

Veit R, Zankl M, Petoussi N, Mannweiler E, Williams G and Drexler G (1989) Tomographic anthropomorphic models, Part I: Construction technique and description of models of an 8-week-old baby and a 7-year-old child. GSF-Report 3/89,GSF-National Research Center for Environment and Health, Neuherberg, Germany

Veit R, Panzer W, Zankl M and Scheurer C (1992) Vergleich berechneter und gemessener Dosen an einem anthropomorphen Phantom. Z. Med. Phys. **2**:123-126

Williams G, Zankl M, Abmayr W, Veit R and Drexler G (1986) The calculation of dose from external photon exposures using reference and realistic human phantoms and Monte Carlo methods. Phys. Med. Biol. **31**:347-354

Xu X G, Chao T C and Bozkurt A (2000) VIP-MAN: An Image-based Whole-body Adult Male Model Constructed From Colour Photographs Of The Visible Human Project For Multi-particle Monte Carlo Calculations. Health Physics **78**(5):476-486

Zankl M, Drexler G, Petoussi-Henss N, Saito K (1997), The Calculation of Dose from External Photon Exposures Using Reference Human Phantoms and Monte Carlo Methods. Part VII: Organ Doses due to Parallel and Environmental Exposure Geometries. GSF-Report 8/97. Institut für Strahlenschutz, GSF-Forschungszentrum für Umwelt und Gesundheit, Neuherberg-Muenchen

Zankl M and Wittmann A (2001) The adult male voxel model "Golem" segmented from whole-body CT patient data. Radiat Environ Biophys. **40**: 153-162

Zankl M, Fill U, Petoussi-Henss N, Regulla D (2002a) Organ dose conversion coefficients for external photon irradiation of male and female voxel models. Phys Med Biol. **47**, No.14, 2367-2386

Zankl M (2002b), Private communication, email from January 18

Zankl M, Petoussi-Henss N, Fill U and Regulla D (2002c), Tomographic anthropomorphic models. Part IV: Organ doses for adults due to idealized external photon exposures, GSF – National Research Center for Environment and Health, Neuherberg, Germany, GSF-Report 13/02

Zubal I G, Harrell C R, Smith E O, Rattner Z, Gindi G and Hoffer P B (1994a) Computerized three-dimensional segmented human anatomy. Med.Phys. 21 No.2, 299-302

Zubal I G, Harrell C R, Smith E O, Smith A L and Krischlunas P (1994b) High resolution, MRI-based, segmented, computerized head phantom. In: The Zubal Phantom Data, Voxel-Based Anthropomorphic Phantoms,http://noodle.med.yale.edu/phantom

Zubal I G, Harrell C R, Smith E O and Smith A L (1995) Two dedicated software, voxel-based, anthropomorphic (torso and head) phantoms. In: Proceedings of an International Workshop on Voxel Phantom Development held at the National Radiological Protection Board,Chilton,UK,6-7 July

Zubal I G (2001) The Zubal Phantom Data, Voxel-Based Anthropomorphic Phantoms. http://noodle.med.yale.edu/phantom